First-principle study of amorphous germanium under pressure

G. Mancini[1]*, *M. Celino*[2], *A. Di Cicco*[1]

[1] *Università di Camerino Via Madonna delle Carceri 62032, Camerino (MC), Italy*

[2] *ENEA, Ente per le Nuove Tecnologie, l'Energia e lo Sviluppo Economico Sostenibile C. R. Casaccia, Via Anguillarese 301, 00123 Roma, Italy*

Abstract. In this paper we present the study of the modifications of structural properties of *a*-Ge due to the application of external pressure. The investigations are carried out in the framework of density functional theory via first-principles molecular dynamics (FPMD).

1 Introduction

Amorphous germanium (*a*-Ge) has been largely studied in the last decades using a variety of experimental and theoretical methods being a material of undisputed importance in basic science and applications in everyday life. Moreover the investigation of the structure of the condensed phases of germanium is of importance for fundamental science since in the solid state it exhibits polymorphism and pronounced changes in density and bonding upon melting and application of external pressure.

Germanium in its stable crystalline phase at room pressure, has a diamond structure (GeI) in which each atom is surrounded by four covalently bonded first neighbors in a tetrahedral formation. This phase of Ge has a very low density with respect to a close-packed structure and is semiconducting. Upon application of pressure, the tetrahedrally bonded network is broken and both the number of neighbors and the density increase. Around 11 GPa, a phase transition to the metallic β-Sn structure (GeII) occurs and even at higher pressures a hexagonal phase and a close-packed phase are found. Recently, an ab-initio metadynamics approach enlightened the existence of an intermediate phase in the lower pressure regime: the mC16 phase with four-membered rings, less dense than diamond [1]. Upon decompression, the crystalline stable structure is not always recovered, rather metastable crystalline phases are observed. The most common one is called ST12 (GeIII). It is based on tetrahedral structure with 12 atom per unit cell arranged to form fivefold and sevenfold rings. In this phase, Ge has higher density (about 10%) than the underlying stable one as reported in Ref. [2]. It is based on tetrahedral structure with

*Corresponding author. E-mail: giorgio.mancini@unicam.it.

12 atom per unit cell arranged to form five-fold and seven-fold rings. As reported in Ref. [3], in case of rapid decompression (about 1 s from the high-pressure phase), a cubic structure characterized by eight atoms per unit cell and called BC8 (or GeIV) is likely to occur [3, 4]. This structure is not stable at room temperature but it transforms to the lonsdaleite structure (hexagonal with four atoms per unit cell) within a few hours.

At room pressure the melting temperature of crystalline Ge is $T_m \simeq 1210$ K. At the melting transition the tetrahedral network is broken and the average coordination number increases from 4 to about 7, which is still low compared to other liquid metals which typically have coordination number between 9 and 12. Liquid Ge is metallic and amorphous Ge is semiconducting. Amorphous Ge is characterized by a continuous random network of distorted defective tetrahedra. Numerous experimental investigations of the density and bonding changes in different phases of germanium are presented in literature, using both x-ray [5] and neutron diffraction [6] techniques. Bond lengths do not differ more than 1% from the crystalline form and bond angles show a modest spread of the order of 10 degrees about the ideal value of the crystalline counterpart. Moreover *a*-Ge shows a complex behavior when an external pressure is applied, and scattered results are reported in literature. In particular, evidence for a sharp drop in resistivity and crystallization of thin *a*-Ge films was found at about 6 GPa [4, 7]. The x-ray absorption spectroscopy (XAS) technique was used to study the evolution of the local structure at high pressures. Freund et al. [8] showed that *a*-Ge remains amorphous up to 8.9 GPa while more recent XAS measurements showed that at 8 GPa *a*-Ge undergoes a phase transition though remaining amorphous [9]. The glass transitions in Ge under pressure was also studied in recent works both experimentally [10, 11] and through molecular dynamic simulations [12]. The combination of Raman and XAS spectroscopy measurements permitted to confirm that 8 GPa marks the onset of a polyamorphic transition in more homogeneous samples [13]. Moreover, Ref. [13] demonstrates that the actual transitions observed in a given sample depend on the initial morphology of the sample. However, the experiments reported in Ref. 17 were done in a limited pressure range (10–12 GPa) and did not account for the transitions occurring upon depressurization.

Polymorphism of amorphous Ge is reported to occur between the low-density amorphous (LDA) semiconductor and the high-density metallic amorphous (HDA) forms. This intriguing phenomenon is linked to a proposed first-order density- and entropy-driven phase transition in the supercooled liquid state [14]. The LDA-HDA transition has been studied in detail for thin film samples by X-ray absorption, extended X-ray-absorption fine structure (EXAFS), and Raman scattering methods [9, 13, 15]. Nevertheless, a detailed and unambiguous understanding of the complex phenomena taking place in *a*-Ge under pressure has only recently published [15].

In this paper, we report the study of the structural properties of *a*-Ge via first-principles molecular dynamics (FPMD) in the framework of density functional theory. We focus on the structural modification due to the application of the external pressure. An amorphous structure is produced by the quench of a melded, disordered structure at high temperature. After a detailed characterization of the amorphous structure in terms of neutron structure factor, pair correlation function and nearest neighbor analysis, the pressure is applied. During compression a room temperature is kept to mimic real experimental conditions.

The pressure is applied to the amorphous structure up to 14 GPa, but in the range 8-10 GPa, in good agreement with experimental results [13], a phase transition is observed. A detailed characterization of the atomic structure provides insights about phase transition under pressure. During the phase transition, the average coordination number goes from 4 for the a-Ge to about 6 of the high pressure phase.

2 Computational details

The first-principles molecular dynamics framework is applied to generate and characterize reliable amorphous structures of Ge. The software employed is CPMD (Car-Parrinello Molecular Dynamics) [16, 17]. The self consistent evolution of the electronic structure during the motion is described within density functional theory. A generalized gradient approximation (BLYP-GGA) is adopted for the exchange and correlation part of the total energy [18, 19] and norm conserving pseudopotentials are used for the core-valence interactions. A Γ-point sampling for the supercell's Brillouin-zone integration has been adopted. As shown for similar systems [20], the choice of the Γ-point sampling demonstrated a reasonable one for a 125-atom model. The electronic wave functions were expanded in plane waves up to the kinetic energy cutoff of 60 Ry and an integration time step of 3 a.u. (0.072 fs) was used.

During the equilibration of the liquid and solid structures a Nosé thermostat was used to control the ion temperature [21, 22, 23]. The characteristic frequency for the thermostat was 1000 cm^{-1}, which lies close to the peak at 37 THz in the diamond phonon density of states [24]. A second Nosé thermostat was used to control the fictitious electronic kinetic energy [25]. This thermostat prevents the electronic wave functions from drifting away from the instantaneous ground state (the Born–Oppenheimer surface), by removing excess fictitious kinetic energy. This drift is particularly severe for metals. In our simulation the liquid Ge sample possesses no band gap and hence the energy transfer rate is high. The characteristic frequency for the thermostat was 45000 cm^{-1} and the target kinetic energy was chosen according to the prescriptions in Ref. [25]. The Noseé thermostat on the electrons was used throughout the simulation and proved to be an effective way of keeping the electrons on the Born-Oppenheimer surface. During the equilibration of the liquid, the cooling of the liquid, and the temporal averaging of the solid, the deviation from the Born–Oppenheimer surface was never more than 0.01 eV/ion, and was often much less. This set of parameters yields accurate and converged properties for Ge crystalline lattices, both diamond and β-Sn.

Amorphous structures have been obtained for a system consisting of N= 125 atoms in periodically repeated cubic cells of size L= 15.61 Å. The starting density is equal to the experimental value for a-Ge at T= 300 K: ρ= 5.51 gr/cm^3 [26]. To ensure that our results are independent on the initial atomic configurations, they are chosen to be drastically different from the crystalline counterpart. Since it is expected that the amorphous structures have a high percentage of Ge atoms four-fold coordinated, the starting configuration has been generated by randomly placing the atoms in the simulation cell. This procedure designs a starting configuration with many defects and many atoms with coordination different from four.

We further disordered the configuration by constant temperature and constant pressure MD equilibration at high temperature (T= 4000 K). During the high temperature simulations, atoms covered a distance as long as about 2 nm ensuring the final configuration retains no memory of the initial geometry. Then we gradually lowered it to T= 1278 K in 10 ps before an additional equilibration for additional 5 ps. The liquid configuration at T= 1278 K, just above the melting temperature, has been used as starting point for the quenching procedure. The amorphous Ge is attained by cooling to 300 K the liquid sample over 0.5 ps. The system was then equilibrated for a further 0.5 ps to gain temporal averages. Two further simulations were performed to study the effect of quench on the atomic structure. One simulation used a slower cooling rate while in the other the liquid was cooled instantaneously to 300 K.

The amorphous structure is then used to produce amorphous structures under pressure. Pressure is applied via the method of Parrinello-Rahman [27] and it is increased by increments of 2 GPa up to 14 GPa. At each pressure the atomic system is relaxed according to the criterion that all the physical quantities are converged.

3 Results

3.1 Amorphous structure

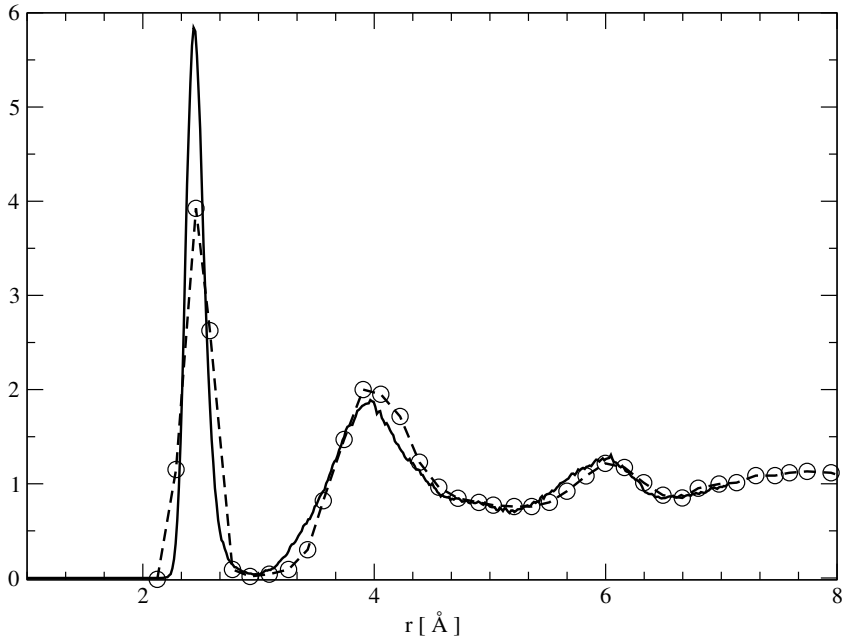

Figure 1: Pair correlation function $g(r)$ of amorphous Ge at T= 300 K. Full line is the first-principle MD, squares is the experiment Ref. [28].

Constant temperature and constant pressure MD simulations are performed to produce an a-Ge via the melt from the quench technique, as discussed in the previous section. The

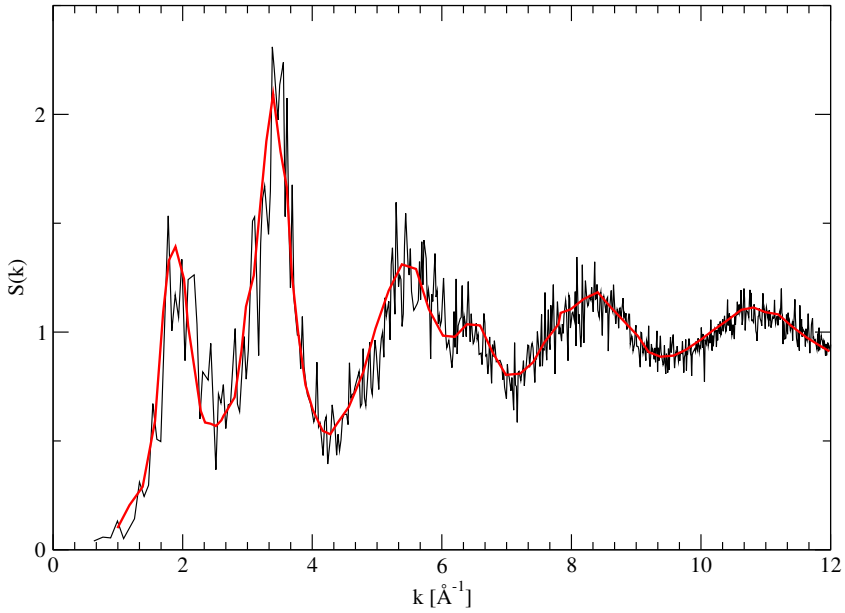

Figure 2: Static structure function S(k) for amorphous Ge at T= 300 K. Full line is the first-principle MD, squares is the experiment Ref. [26].

good agreement of the calculated $g(r)$ and $S(q)$ (Figs. 1 and 2) confirms the reliability of our method.

Moreover the comparison with experiments confirms us that we have produced a good starting point for the simulations of a-Ge under an external pressure. The computer generated amorphous sample is slightly overcoordinated (N= 4.05), indicating that 5-fold coordinated defects are somewhat more frequent than threefold coordinated sites. Further annealing process increase the agreement with experiment in terms of $g(r)$ and $S(q)$ but not in the reduction of the number of defects.

In Fig. 1 the computed pair correlation function is compared with the experimental result from Ref. [28]. There is an overall agreement for what concern both the position of the peaks and their heights. The reliability of our amorphous sample is confirmed by the good agreement between computed total structure factor and the experimental one, on the entire range of k values (Fig. 2).

3.2 LDA-HDA transition

Having verified the reliability of the amorphous configuration at zero pressure, an external pressure has been gradually applied to the atomic system. Each time, the simulation is long enough to allow the system to relax all internal degrees of freedom and to find the volume at equilibrium at each pressure. As shown in the pressure–volume curve given in Fig. 4, the volume changes smoothly up to 8 GPa and at this pressure an abrupt decline of the volume is seen, indicating a phase transition. The volume drop is close to the peculiar change already obtained in diamond to β–Sn transformation from c-Ge. Amorphous Ge

transforms from a low-density amorphous phase into a metallic high density phase: the good agreement with experimental results [13], despite the finite size of the simulation cell, is mainly due to the long time scales attained to allow complete equilibration of the atomic systems.

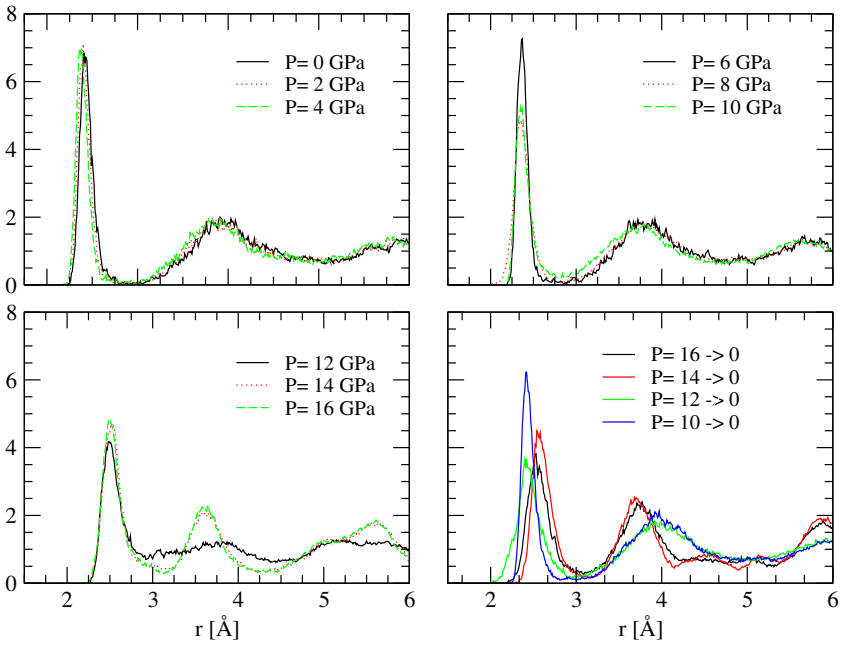

Figure 3: Comparison of the pair correlation functions for different values of the external pressure.

Zero-pressure sample upon rapid decompression is still an amorphous structure, denser than the initial structure because of the volume drop at the transition. Thus we can argue that the path on pressure release is reversible. The structure is found to be denser than the initial amorphous structure, indicating that an irreversible amorphous to amorphous phase transition has been seen.

As for the coordination number, at zero pressure it is centered around the crystalline one. An high percentage of atoms, about 92.8%, has coordination four. Upon application of the pressure the percentage of atoms with coordination 4 lowers and the distribution is slightly broader. At 8 GPa the percentage of atoms with coordination 4 is only 84.6% and there is evidence of 5-fold coordinated atoms (14.6%). During the phase transformation, at 10 GPa, the 4-fold coordinated atoms are about 68% and increase even more the 5-fold coordinated atoms (29.1%). At 12 GPa a new phase appears, as shown by the coordination number, in which 4-fold and 5-fold coordinated atoms are only 1.2% and 13.1%, respectively. On the contrary, percentages of 6-fold, 7-fold, 8-fold coordinated atoms are 41.3%, 33.3% and 10.1%, respectively. Thus the phase transition is characterized by a broader distribution of coordinations centered on coordination 6. Upon decompression partially lower coordination numbers are recovered and the 5-fold coordinated atoms are 49.3%.

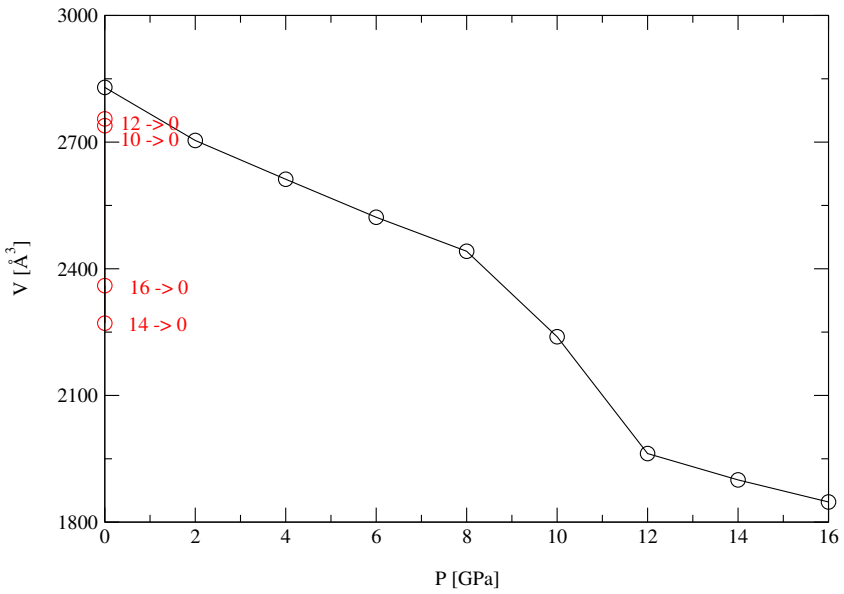

Figure 4: Cell volume versus external pressure. Loading of the pressure up to 16 GPa and unloading in one shot to zero pressure.

4 Conclusions

We showed that structural information gathered from molecular dynamics are able to provide an atomic-scale description of the phase transformation under pressure. This leads to a clear picture of the topological differences between systems having the same composition but different chemical nature and systems made of the same species but differing in composition.

The present approach finally provides a general framework for establishing bonding constraints in a neat way via model simulations, and will be used in the future for establishing constraint counting algorithms in more complex glassy materials from Molecular Dynamics.

5 Acknowledgements

The calculations were performed by using facilities and services available in the ENEA GRID infrastructure (Italy).

References

[1] Selli D., Baburin I. A., Martnak R., and Leoni S. *Scientific Reports*, 3:1466, 2013.

[2] Bundy F. and Kasper J. S. *Scientific Reports*, 139:340, 1963.

[3] Nelmes R. J., McMahon M. I., Wright N. G., Allan D. R., and Loveday J. S. *Phys. Rev. B*, 48:9883, 1993.

[4] Shimomura O., Minomura S., Sakai N., Asaumi K., Tamura K., Fukushima J., and Endo H. *Philos. Mag*, 29:547, 1974.

[5] Filipponi A. and Di Cicco A. *Phys. Rev. B*, 51:12322, 1995.

[6] Salmon P. S. *J. Phys. F: Met. Phys.*, 18:234, 1988.

[7] Tanaka K. *Phys. Rev. B*, 43:4302, 1991.

[8] Freund J., Ingalls R., and Crozier E. D. *J. Phys. Chem.*, 94:1087, 1990.

[9] Principi E., Di Cicco A., Decremps F., Polian A., De Panfilis S., and Filipponi A. *Phys. Rev. B*, 69:201201(R), 2004.

[10] Hedler A., Klaumunzer S. L., and Wesch W. *Nature Mater.*, 3:804, 2004.

[11] Bhat M. H., Molinero V., Soignard E., Solomon V. C., Sastry S., Yarger J. L., and Angell C. A. *Nature (London)*, 448:787, 2007.

[12] Kga J., Nishio K., Yamaguchi T., and Yonezawa F. *J. Phys. Soc. Jpn.*, 73:388, 2004.

[13] Di Cicco A., Congeduti A., Coppari F., Chervin J. C., Baudelet F., , and Polian A. *Phys. Rev. B*, 78:033309, 2008.

[14] Barkalov O. I., Tissen V. G., McMillan P. F., Wilson M., Sella A., and Nefedova M. V. *Phys. Rev. B*, 82:020507(R), 2010.

[15] Coppari F., Chervin J. C., Congeduti A., Lazzeri M., Polian A., Principi E., and Di Cicco A. *Phys. Rev. B*, 80:115213, 2009.

[16] Cpmd v3.13.2 copyright ibm corp 1990-2008, copyright mpi für festkörperforschung stuttgart 1997-2001.

[17] Andreonia W. and Curioni A. *Parallel Computing*, 26:819–842, 2000.

[18] Becke A. D. *Phys. Rev. B*, 38:3098, 1988.

[19] Lee C. L., Yang W., and Parr R. G. *Phys. Rev. B*, 37:785, 1988.

[20] Celino M. and Massobrio C. *Phys. Rev. Lett*, 90:125502, 2003.

[21] Parrinello M. and Rahman A. *J. Appl. Phys.*, 52:289, 1981.

[22] Nosé S. *Mol. Phys.*, 52:255, 1984.

[23] Nosé S. *J. Chem. Phys*, 81:511, 1984.

[24] Bilz H. and Kress K. *Phonon Dispersion Relations in Insulators.* Springer, Berlin, 1979.

[25] Bl ochl P. E. and Parrinello M. *Phys. Rev. B*, 45:9413, 1992.

[26] Waseda Y. *The structure of non-crystalline materials - liquids and amorphous solids.* McGraw-Hill, New York, 1981.

[27] Parrinello M. and Rahman A. *Phys. Rev. Lett.*, 45:1196, 198.

[28] Etherington G., Wright A. C., Wenzel J. T., Dore J. C., Clarke J. H., and Sinclair R. N. *J. Non-Cryst. Solids*, 48:265, 1982.